SCIENTIFIC REPORTS

OPEN

Regeneration associated transcriptional signature of retinal microglia and macrophages

Diana M. Mitchell [1], **Chi Sun**[1,2], **Samuel S. Hunter**[3], **Daniel D. New**[3] & **Deborah L. Stenkamp**[1]

Zebrafish have the remarkable capacity to regenerate retinal neurons following a variety of damage paradigms. Following initial tissue insult and a period of cell death, a proliferative phase ensues that generates neuronal progenitors, which ultimately regenerate damaged neurons. Recent work has revealed that Müller glia are the source of regenerated neurons in zebrafish. However, the roles of another important class of glia present in the retina, microglia, during this regenerative phase remain elusive. Here, we examine retinal tissue and perform QuantSeq. 3′mRNA sequencing/transcriptome analysis to reveal localization and putative functions, respectively, of *mpeg1* expressing cells (microglia/macrophages) during Müller glia-mediated regeneration, corresponding to a time of progenitor proliferation and production of new neurons. Our results indicate that in this regenerative state, *mpeg1*-expressing cells are located in regions containing regenerative Müller glia and are likely engaged in active vesicle trafficking. Further, *mpeg1*+ cells congregate at and around the optic nerve head. Our transcriptome analysis reveals several novel genes not previously described in microglia. This dataset represents the first report, to our knowledge, to use RNA sequencing to probe the microglial transcriptome in such context, and therefore provides a resource towards understanding microglia/ macrophage function during successful retinal (and central nervous tissue) regeneration.

Microglia are resident immune cells of the macrophage lineage present in the vertebrate central nervous system (CNS). Recent work has identified crucial microglia-mediated functions in CNS development and maintenance[1–8], substantially increasing our understanding of essential, intricate, and regulated interactions of microglia with neurons and with other glia in healthy CNS tissue. In contrast, in some contexts, microglia appear to contribute to pathology in neurodegenerative disease[9,10]. There is currently a lack of information regarding the function of microglia and microglia-derived factors, and that of any other immune cells present, in contexts of successful CNS (including retinal) regeneration, which occurs in non-mammalian vertebrates such as zebrafish. Further, limited markers currently exist to identify microglia and macrophages in zebrafish CNS tissue, although many reports support the zebrafish as a model for microglial biology[11–15]. Collectively, this limits our understanding of regenerative mechanisms, requirements for successful CNS regeneration, and regulation of an environment conducive to regeneration.

Our current understanding of retinal regenerative mechanisms is based largely upon the zebrafish model, and arises from the study of important roles of Müller glia (MG), rather than microglia. Following a variety of distinct damage paradigms resulting in death of retinal neurons in zebrafish, MG act as the source of new neurons in regenerated retinal tissues[16–21]. Gene expression and proteomic studies of retinal tissue during retinal regeneration in zebrafish have improved our understanding of this regenerative process[22–24], but these studies did not differentiate between cell types contributing to transcript/protein abundance. Gene profiling studies of MG-derived progenitors have more specifically revealed transcriptional changes within this cell type in response to damage[25], and have identified intrinsic factors required for regeneration shared by other regenerating tissues[26]. MG are also present in the mammalian retina; however, rather than regenerating neurons following injury or damage, a state of gliosis ensues[27–29]. Gliotic tissue is associated with hallmarks of inflammation, reactive microglia, and may result in glial scarring[27,28,30]. Interestingly, zebrafish mount a substantial microglia/macrophage response to a widespread retinal tissue lesion with inflammatory characteristics that is subsequently followed by successful

[1]Department of Biological Sciences, University of Idaho, Moscow, ID, 83844, USA. [2]Present address: Ophthalmology, Washington University in St. Louis, 4523 Clayton Ave St. Louis, Missouri, 63110, USA. [3]Institute for Bioinformatics and Evolutionary Studies, University of Idaho, Moscow, ID, 83844, USA. Correspondence and requests for materials should be addressed to D.M.M. (email: dmitchell@uidaho.edu)

neuronal regeneration[31] and zebrafish reportedly display transient characteristics of gliosis[32,33]. Further, immune cell-MG crosstalk may shape MG reaction to retinal injury[34–36], and possibly have effects on MG-mediated retinal regeneration[37]. Interestingly, a relatively recent study performed RNA sequencing of zebrafish MG-associated transcripts at early timepoints following light damage and found enrichment of genes categorized within cytokine signaling and immunity[25]. Recent reports have demonstrated FACS-based isolation of microglia and macrophage populations from other cell types in dissociated zebrafish CNS tissue for downstream RNA sequencing[12,38–40]. This has facilitated our understanding of the characteristics of zebrafish CNS microglia. However, such an analysis of microglia isolated from tissue engaged in a regenerative response in the CNS is necessary to better inform our understanding of microglia/macrophage contribution to CNS health and disease.

In zebrafish, a characteristic sequence of events follows retinal tissue injury. Upon death of retinal neurons, phagocytic cells (including microglia/macrophages and Müller glia) engulf debris arising from tissue insult[31,41,42]. A proliferative phase next ensues in which Müller glia re-enter the cell cycle and generate proliferative neuronal progenitors[16,18,19,21,31,43–45]. These progenitors then exit the cell cycle and differentiate to neurons resulting in regeneration of lost neuronal cell types[18,19,43,46,47], and recovery of retinal tissue function[21,43,48].

We previously reported that microglia and extra-retinally derived macrophages initially mount a robust response to widespread neuronal death induced by the neurotoxin ouabain[31]. This initial response is followed by a transition to MG proliferation[18,31]. Here, we investigate microglia/macrophage presence and characteristics during the subsequent phase involving MG-derived retinal regeneration. It is at this stage that zebrafish display a regenerative outcome, whereas mammals instead enter a phase corresponding to a gliotic response. Since microglia, and often other immune cells, participate in this gliotic response in mammals, we sought to reveal microglia/macrophage characteristics during active MG-mediated retinal regeneration in zebrafish. To this end, we examined localization of immune cells in regenerative retinal tissue and sequenced their mRNA transcriptome in this context. We find that immune cells present in regenerating tissue identify as microglia/macrophages based on expression of *mpeg1*-driven GFP[13,49] and that microglia/macrophages in regenerating tissue show altered spatial distribution with congregations of microglia/macrophages localized to the optic nerve head and surrounding regions. To reveal the gene expression program of microglia/macrophages in such a context, we performed QuantSeq. 3'mRNA transcriptome analysis of *mpeg1*:GFP+ cells isolated from regenerating retinas and identified several novel genes not previously described in microglia, as well as a list of transcripts associated with *mpeg1*-expressing cells during retinal regeneration. We generated a list of candidate "regeneration-associated" transcripts, which showed enrichment of Gene Ontology categories suggesting increased vesicle trafficking within *mpeg1* expressing cells during retinal regeneration. This transcriptome data set provides a wealth of interesting and novel genes to be considered for follow-up studies towards identifying microglia/macrophage function during zebrafish retinal regeneration.

Results

Features of immune cells and Müller glia in regenerating retinal tissue.
Recent studies have begun to reveal characteristics of microglia, including observations of their identity and features in retinal tissues, during MG reactivity and resulting retinal regeneration in zebrafish following neuronal damage[31,37]. To build on this foundation, we visualized localization and characteristics of immune cells (including microglia) in retinal tissue undergoing active regeneration following a tissue-disrupting lesion. We analyzed cryosections at seven days following intravitreal injection of a final concentration 2 μM of ouabain (7 dpi). This lesioning strategy has been shown to destroy inner retinal neurons, but to spare photoreceptors and MG[18,21,31,48]. The 7 dpi timepoint follows the initial response to tissue injury (which peaks approximately 1–2 dpi[18,31]) as well as the shift to the proliferative phase in which MG have re-entered the cell cycle (approximately 3 dpi). By 5 dpi, neuronal progenitors are detected[18] and by 7 dpi, MG-derived progenitors begin to enter the regenerative phase[18,19] as evidenced by detection of ganglion cell markers[18,21], as well as markers of ganglion cell axon outgrowth[18].

To visualize microglial, and any other immune cell, features in this regenerative state, we used an antibody to L-plastin, which marks all immune cells including microglia[31,50,51], and an antibody to glutamine synthetase (GS) to label MG. We observed that L-plastin+ cells were present within regenerating retinal tissue containing reactive GS-labeled MG within regions of the inner retina corresponding to the location of the initial retinal lesion (Fig. 1B,B',B"). At 7 dpi, L-plastin+ cells appeared predominantly localized to this damage-specific region within the inner retina (Fig. 1B). Müller glia displayed hypertrophy (Fig. 1B,B',B", compared to Fig. 1A,A'), consistent with previous observations following a variety of damage paradigms[18,21,32].

L-plastin+ cells in regenerating retinas were irregularly distributed throughout the retinal tissue (Fig. 1B,D), rather than showing a more evenly spaced distribution as in control retinas (Fig. 1A,C), and in contrast to that seen in acutely damaged ouabain injected retinas[31]. L-plastin+ cells within the regenerating retina appeared to predominantly localize to the basal portions of the regenerating inner retina, while only rarely seen to be localized to apical regions corresponding to Müller glia-derived neuronal progenitor proliferation[19,52] (Figs 1–3). The L-plastin+ cells were not ramified and instead were irregular in shape (Figs 1B,B',B" and 2D–F).

We also observe that L-plastin+ cells appeared most densely present in regions corresponding to, and surrounding, the optic nerve head (onh, Fig. 1B,D) in regenerating retinas, and density of L-plastin+ cells was reduced in a gradient as a function of distance from the onh (Fig. 1A–D). Further, many L-plastin+ cells were visible in tissues apical to the retina and were directionally (radially) oriented towards retinal tissue (Fig. 1B',B", arrows). It is possible that these apically positioned L-plastin+ cells may represent RPE-associated microglia that migrate into the regenerating retina, or possibly extra-retinally derived immune cells that continue to infiltrate the retina beyond the previously documented timepoint of 3 dpi[31]. L-plastin+ cells within retinal tissue at 7 dpi ouabain or saline co-labeled with the macrophage-specific *mpeg1*-driven GFP transgene (Fig. 2), therefore indicating that these immune cells consist of microglia[13] and possibly other infiltrating macrophages.
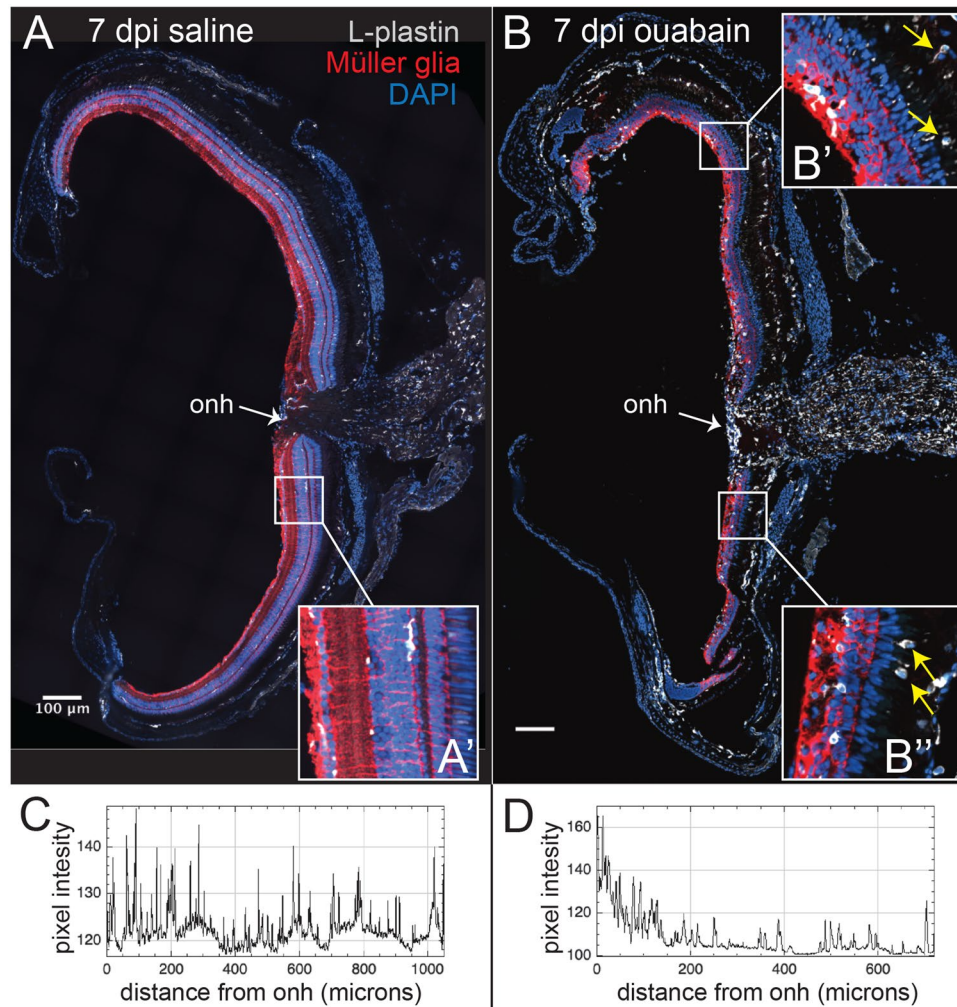
Figure 1. Immune cell features and distribution in regenerating retinal tissue. Images show retinal cryosections at 7 days post injection (7 dpi) of saline (**A**) or $2\,\mu M$ final concentration of ouabain (**B**) stained for L-plastin (gray; microglia/macrophages), Glutamine Synthetase (GS, red; Müller glia), and DAPI (blue; nuclei). A and B show stitched images of entire cryosections, insets (A', B', and B") show indicated enlarged regions. Müller glia in retinas 7 dpi ouabain display hypertrophy throughout the regenerating inner retina and appear disorganized (B',B") compared to control (A'). (**C,D**). Plots show pixel intensity of L-plastin+ signal as a distance from the optic nerve head (onh). L-plastin+ cells in saline injected retinas show even distribution and are ramified (A, A',C), while L-plastin+ cells in regenerating retinas (B-B") appear irregularly dispersed (**D**) and display ameboid morphology. B' and B" reveal that the L-plastin+ cells in the inner retina conform to the network of Müller glial cells labeled by GS expression. In addition, L-plastin+ cells are densely localized in regions corresponding to the optic nerve head (onh) at 7 dpi ouabain, and several immune cells appear in regions apical to the retina with directional orientation that could suggest migration into retinal tissue from the RPE or outside of the retina (yellow arrows, B' and B"). Scale bars in (**A,B**) = 100 μm.

Since 7 dpi corresponds to near-peak numbers of cells expressing PCNA[18], we stained and imaged cryosections of regenerating retina to visualize PCNA in combination with L-plastin and GS (Fig. 3) to determine if any L-plastin+ cells express PCNA. PCNA signal was not detected in tissue at 7 dpi following saline injection (Fig. 3A,B). As previously reported[18], PCNA signal was detected throughout the inner retina at 7 dpi following ouabain injection, often found in clusters, and nuclei with PCNA signal adopted an elongated shape (Fig. 3C–F). We observe that most of the nuclei containing PCNA at 7 dpi ouabain were associated with GS-labeled cytoplasmic signal (Fig. 3D). Occasionally, PCNA signal was associated with L-plastin+ cytoplasm, but this often overlapped with GS signal (Fig. 3D–F, arrows), making it difficult to attribute proliferation to MG (GS+) versus L-plastin+ cells. Collectively, this indicates that PCNA expression at this timepoint primarily represents reactive MG and MG-derived progenitors.

Transcriptome analysis of *mpeg1*:GFP+ cells during retinal regeneration. Since functions of immune cells, including microglia, in the context of successful retinal (or CNS) regeneration are not well understood, and to build on previous gene expression studies during zebrafish retinal regeneration[22,23,25], we sought to
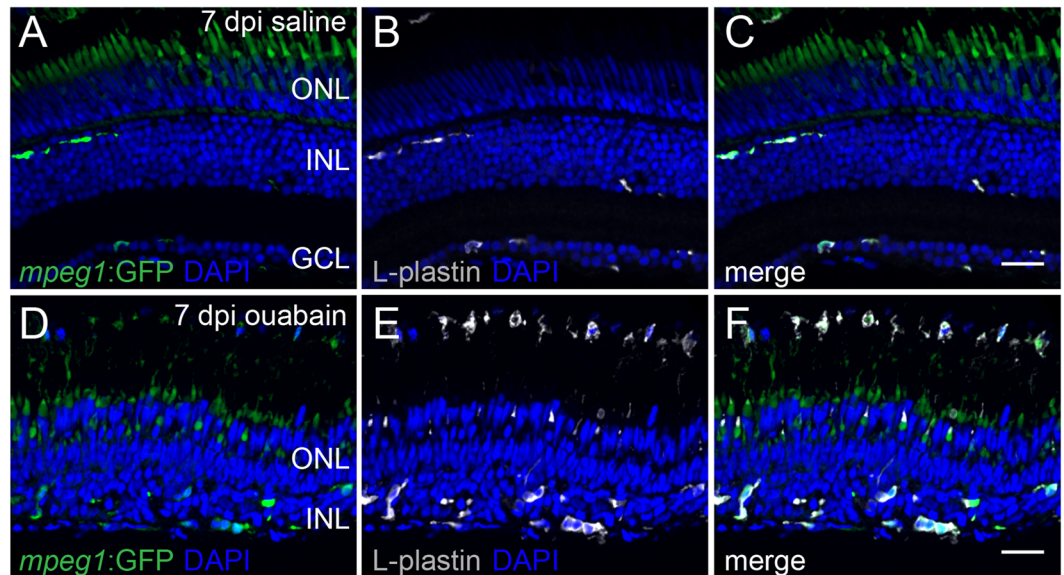
Figure 2. L-plastin+ cells in regenerating retinal tissue co-label with *mpeg1*-driven GFP. Images of a retinal cryosection at 7 dpi saline (**A–C**) or ouabain (**D–F**) injection obtained from *mpeg1*:GFP transgenic fish and visualized for *mpeg1*:GFP (green, **A,D**), L-plastin immunolabeling (gray, **B,E**), and DAPI staining (blue; nuclei, **A–F**). (**C,F**) Three color merge. L-plastin+ cells co-label with the *mpeg1*:GFP transgene. Autofluorescence from photoreceptors is visible in the outer nuclear layer (ONL) in other channels (**A,C,D,F**) in fixed cryosection images, however, this autofluorescence did not affect FACS sorting of GFP+ and GFP− populations from freshly isolated, dissociated regenerating retinas. Scale bar in (**C,F**) = 20 μm apply to (**A–F**). ONL: outer nuclear layer, INL: inner nuclear layer, GCL: ganglion cell layer.

identify the microglia (and macrophage)-specific transcriptome corresponding to an environment of successful regeneration, to gain insight into those possible functions. As described above, L-plastin+ cells localized within retinal tissue obtained from *mpeg1*:GFP transgenic zebrafish at 7 dpi co-labeled with *mpeg1*-driven GFP (Fig. 2). *Mpeg1*-driven GFP expression allowed us the opportunity to use GFP signal as a basis to isolate GFP+ microglia/macrophages[13,49] from other retinal cell types (GFP−) during active retinal regeneration, followed by QuantSeq. 3′-mRNA sequencing, to reveal their respective transcriptomes (Fig. 4).

We used Fluorescence Activated Cell Sorting (FACS) to isolate highly pure populations of GFP+ and GFP− cells from dissociated cell suspensions from *mpeg1*:GFP transgenic retinas at 7 days post ouabain lesion followed by RNA isolation[38] and (Fig. 4). The results of this dissociation, cell sorting, confirmation of purity, and RNA quality were reported in[38]. To identify the mRNA transcripts present in *mpeg1*:GFP+ cells compared to GFP− cells during zebrafish retinal regeneration, we performed QuantSeq. 3′-mRNA sequencing of RNA isolated from the sorted GFP+ and GFP− cells. Sequencing of GFP− cells was also included in this experiment in order to compare transcript expression in non-microglial/macrophage populations at this timepoint. Comparison of transcripts between such populations is useful because very little is known about the zebrafish microglia/macrophage transcriptome, and such insight will increase our understanding of these cell types in the zebrafish model organism. Using criteria of moderated log2FC > |2| and FDR < 0.01, we identified 2779 differentially expressed genes, with 970 of these significantly enriched in GFP+ cells (Fig. 4B, Table 1 and Supplementary File S2) and 1809 of these significantly enriched in GFP− cells (Fig. 4B, Table 2 and Supplementary File S2). Principal Component Analysis showed that the sorted GFP+ and GFP− populations formed two highly distinct clusters, indicating that these populations contain distinct transcripts representing different gene expression programs (Supplemental Fig. S1). A heat map was generated based on rlog transformed values of differentially expressed genes with p < 0.1 to broadly illustrate differential expression of transcripts relative to each population (Fig. 4C). This heat map reveals a minor cluster of genes with similar expression levels between GFP+ and GFP− populations, as well as clusters of genes with relatively different expression levels, and reveals only slight variation among samples within groups.

To confirm the output of this design, we probed our data set for selected transcripts in GFP+ and GFP− populations that represent microglia/macrophages and other retinal cell types, respectively. Transcripts pertaining to genes expressed by the monocyte (*spi1a, csf1ra, csf1rb*[53–55]) and macrophage lineages *(mhc2dab, marco,* and *mfap4*[56,57]), and transcripts expressed by microglia (*p2ry12, sall3a, slc7a7*[58–63]), were significantly enriched in GFP+ samples based on Differential Expression and raw counts (Fig. 4E, Table 1, and Supplementary File S1). Importantly, GFP+ populations were enriched for the macrophage/microglia-specific gene *mpeg1.1* as well as *egfp* transcripts, which formed the basis of our FACS sorting (Fig. 4E and Table 1). On the other hand, genes expressed by photoreceptors, including those involved in photoreceptor identity and function (e.g. *crx, opn1lw2, arr3a, rcvrn2, gngt2a, syt5a*[64–70]), were highly enriched in the GFP− population and only minimally detected in the GFP+ population (Fig. 4D, Table 3, and Supplementary File S1), consistent with previous reports that photoreceptors survive the inner retina-selective ouabain lesion[18,21,31,48]. Genes expressed by neuronal progenitors (e.g.
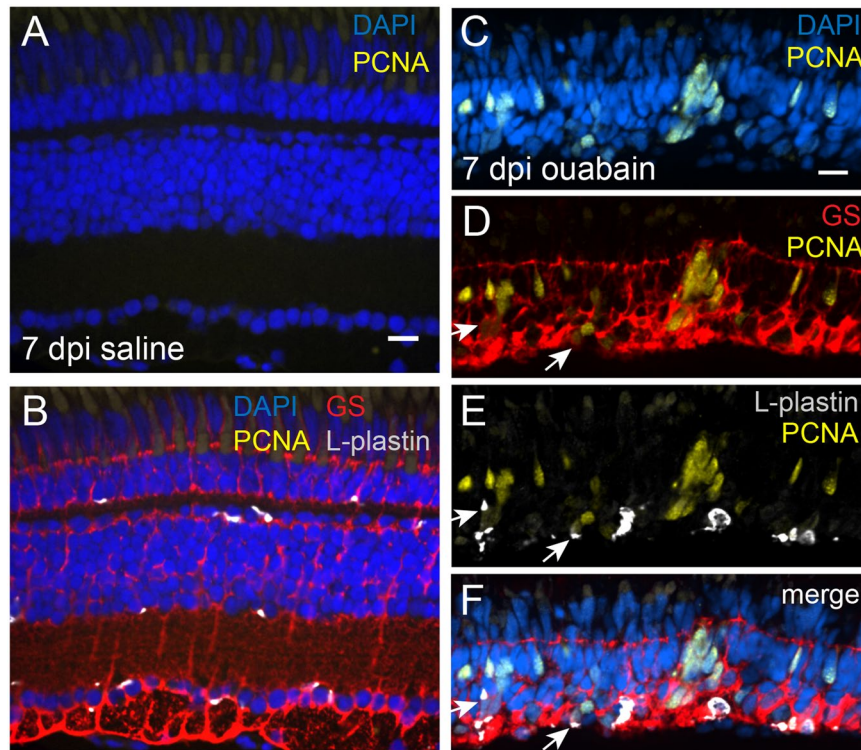
Figure 3. PCNA expression in regenerating retinal tissue at 7 days post ouabain injection. Images of a retinal cryosection at 7 dpi saline (**A,B**) or ouabain injection (**C–F**) stained for DAPI (blue; nuclei), PCNA (yellow), Glutamine Synthetase to mark Müller glia and Müller glia-derived progenitors (red), and L-plastin to mark immune cells (gray). (**A,C**) DAPI and PCNA stain. (**D**) GS and PCNA stain. (**E**) L-plastin and PCNA stain. (**B,F**) Four color merge. In regenerating retinal tissue, cells expressing PCNA cels are visible throughout the inner retina, corresponding to regions of initial tissue damage, and often appear in clusters. Most PCNA signal can be attributed to cytoplasm containing GS signal. Occasionally, PCNA signal is associated with L-plastin+ cytoplasm (**E**), but this often overlaps with GS signal (arrows, **D–F**). Scale bar in A = 10 μm, applies to (**A,B**). Scale bar in C = 10 μm, applies to (**C–F**).

vsx2, *neurod1*, *neurod4*, and *pax6a*[33]) were also highly enriched in the GFP− population (Fig. 4D, Table 2, and Supplementary File S2), consistent with engagement of a regenerative state. Müller glia-associated *gfap* expression was also significantly enriched in GFP− cells, as well as other genes upregulated in Müller glia during zebrafish retinal regeneration (such as *mdka* and *ascl1a*[71–74]) (Fig. 4D, Table 2, Supplementary File S2). In addition, several members of the Notch family (e.g. *notch1b*, *notch3*, *jag1b*, *dla*) were enriched in GFP− populations, consistent with a role for Notch signaling in regeneration of retinal neurons in zebrafish[75–77] (Table 2, Supplementary File S2).

Several selected transcripts identified in the RNA-seq experiment as differentially expressed in GFP+ microglia/macrophages were confirmed by qPCR analysis of GFP+ and GFP− populations sorted from *mpeg1*:GFP+ retinas at 7 dpi in a separate experiment (Tables 3 and 4). Transcripts associated with leukocytes and macrophages (*lcp1* and *mpeg1.1*, respectively[49,50], previously reported to be selectively amplified in the GFP+ sorted population subject to RNA-seq[38]) and microglia (*p2ry12*[62]) were confirmed to be enriched in GFP+ populations compared to GFP− populations (Table 3). We also confirmed that several complement factors identified in the RNA-seq (*c1qa*, *c1qb*, *cfp*, and the complement receptor subunit *itgb2*) were selectively amplified from GFP+ populations (Table 3). In addition, as indicated by the RNA-seq experiment, we also found *apoc1*, *il1b*, and *lgals3bpb* to be enriched in *mpeg1*:GFP+ cells compared to GFP− cells by qPCR (Table 3).

Further consistent with our RNA-seq experiment, transcripts associated with photoreceptors (*crx*, *opn1lw2*) were confirmed to be enriched in GFP− populations using qPCR (Table 4), consistent with the survival of photoreceptors in this damage system[18,21,31,48]. Transcripts expressed by Müller glia and Müller glia-derived progenitors during retinal regeneration (*gfap*, *pax6a*, *ascl1a*[20,74]) were confirmed to be enriched in the GFP− population by qPCR analysis (Table 5). Several other transcripts (*mef2ca*, *ncam1b*, *sept8b*, *pdca*, *prom1b*) found to be enriched in GFP− compared to GFP+ cells in the RNA-seq experiment showed a similar result when analyzed by qPCR (Table 4).

We performed Gene Ontology (GO) and Kegg Pathway analyses of transcripts enriched in the GFP+ population for genes with log2FC > 0 and FDR < 0.1 (Supplementary File S3). Biological Processes overrepresented in GFP+ populations (all reported here with p < 0.01) include categories that are consistent with a microglia/macrophage identity (for example, (innate) immune response, antigen processing and presentation, microglia differentiation, phagocytosis, and respiratory burst). Interestingly, Biological Process categories overrepresented
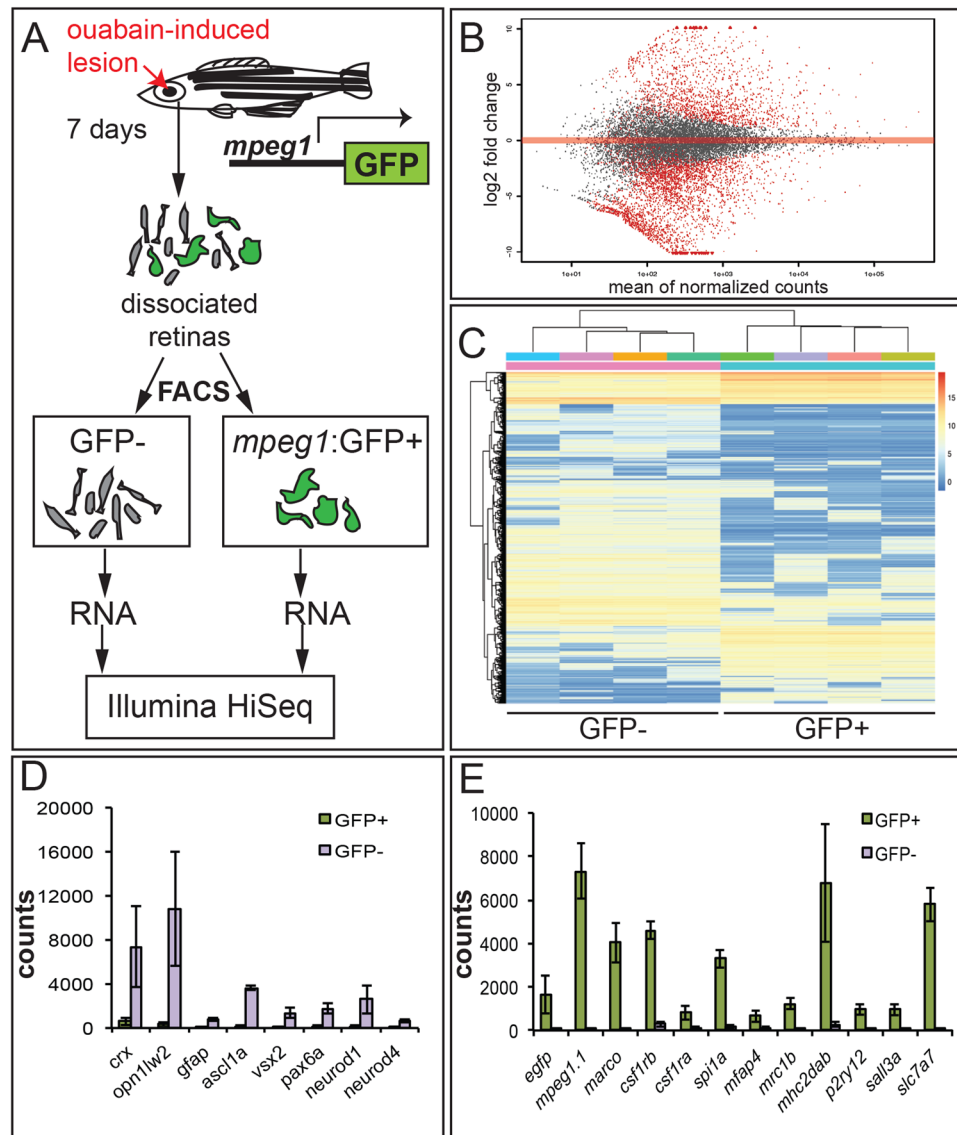
Figure 4. Overview of RNA-sequencing of *mpeg1*:GFP+ and GFP− populations isolated from regenerating retinas. (**A**) At 7 days post ouabain lesion (7 dpi), retinas from *mpeg1*:GFP+ fish were dissociated and subjected to Fluorescence Activated Cell Sorting (FACS) to obtain purified populations of GFP+ and GFP− cells, RNA was isolated from respective populations, and then sequenced by Illumina HiSeq. (**B**) MA plot of moderated Log2 fold change obtained from RNA sequencing. (**C**) Heat map showing row centered rlog transformed values for all genes differentially expressed with p < 0.1, to illustrate expression relative to each (GFP− or GFP+) population. The legend in upper right indicates transcript abundance relative to the other population. (**D**) Raw counts of sequences mapped to genes associated with photoreceptors (*crx*, *opn1lw2*, which survive the retinal lesion), and Müller glia and neuronal progenitors (*gfap*, *ascl1a*, *vsx2*, *pax6a*, *neurod1*, *neurod2*) in GFP+ and GFP− samples. E. Raw counts of sequences mapped to genes associated with *egfp*, macrophages (*mpeg1.1*, *marco*, *csf1a*, *csf1b*, *spi1a*, *mfap4*, *mrc1b*, *mhc2dab*), and microglia (*p2ry12*, *sall3a*, *slc7a7*) in GFP+ and GFP− populations. Error bars in (**D**,**E**) represent SEM.

in GFP+ cells also include wound healing and categories representing cellular motility and mobility (for example, Arp2/3 complex-mediated actin nucleation, macrophage chemotaxis, regulation of cell migration, positive regulation of actin filament polymerization). Cellular Component categories reflect the intracellular compartments required for microglia and macrophage-mediated digestion of engulfed material (for example, vacuole, vacuolar membrane, lysosome, lysosomal membrane, endocytic vesicle, early endosome, late endosome membrane, autophagosome, vesicle, V-type ATPAse categories) and the location of many innate immune receptors involved in initiating immune responses (for example, cytoplasm, NLRP3 inflammasome complex, AIM2 inflammasome complex, extrinsic component of (cytoplasmic side of plasma) membrane). Molecular Function categories reflect the myriad of enzymes involved in degradation of engulfed material in various cellular compartments (for example, hydrolase activity, alpha-mannosidase activity, ribonuclease T2 activity, catalytic activity acting on a protein, epoxide hydrolase activity), and chemokine activity. Kegg pathway analysis again reflected phagocytosis

moderated log2FC	FDR	GENE NAME	SYMBOL	ZFIN	ENTREZID
6.947697132	8.29E-48	apolipoprotein C-I	apoc1	ZDB-GENE-030131-1074	570638
6.935549678	1.21E-38	solute carrier family 43, member 3b	slc43a3b	ZDB-GENE-060312-28	556206
9.744245899	2.75E-37	regulator of G protein signaling 18	rgs18	ZDB-GENE-061013-722	768164
8.364686368	9.84E-37	chemokine (C-C motif) ligand 34b, duplicate 1	ccl34b.1	ZDB-GENE-091204-276	563952
9.292757461	1.03E-36	hepatitis A virus cellular receptor 1	havcr1	ZDB-GENE-040718-131	436707
5.714666395	2.75E-36	lectin, galactoside-binding, soluble, 9 (galectin 9)-like 1	lgals9l1	ZDB-GENE-030131-9543	337597
10.82966572	4.22E-34	uncharacterized LOC100150882	LOC100150882	NA	100150882
6.712331301	6.09E-32	CD74 molecule, major histocompatibility complex, class II invariant chain b	cd74b	ZDB-GENE-990910-10	30645
5.887950241	4.26E-30	CD74 molecule, major histocompatibility complex, class II invariant chain a	cd74a	ZDB-GENE-000901-1	58113
8.897462506	2.20E-29	solute carrier family 7 (amino acid transporter light chain, y+ L system), member 7	slc7a7	ZDB-GENE-051127-5	641560
6.139928731	1.38E-28	si:busm1-266f07.2	si:busm1-266f07.2	ZDB-GENE-030616-436	368878
8.549659679	6.09E-27	interleukin 10 receptor, alpha	il10ra	ZDB-GENE-070905-4	777651
8.850007997	6.13E-26	integrin, alpha E, tandem duplicate 1	itgae.1	ZDB-GENE-131121-125	100333951
8.699101471	1.84E-25	si:ch73-203a8.1	si:ch73-203a8.1	ZDB-GENE-070912-335	100151151
10.15171232	1.04E-24	protein NLRC3-like	LOC100334101	NA	100334101
8.913425562	1.79E-24	interleukin-1 receptor type 2	LOC101882195	NA	101882195
5.61985783	1.81E-24	complement component 1, q subcomponent, B chain	c1qb	ZDB-GENE-040801-223	445088
6.670581809	3.36E-24	G0/G1 switch 2	g0s2	ZDB-GENE-081022-103	568476
6.506472448	5.92E-24	retinol binding protein 2a, cellular	rbp2a	ZDB-GENE-020320-2	568032
4.928284874	1.57E-23	profilin 1	pfn1	ZDB-GENE-031002-33	799355
6.183866184	2.84E-23	lymphocyte cytosolic protein 1 (L-plastin)	lcp1	ZDB-GENE-991213-5	30583
8.504782713	7.69E-22	macrophage receptor with collagenous structure	marco	ZDB-GENE-120514-2	571584
6.059783514	7.69E-22	granulin 1	grn1	ZDB-GENE-060103-1	553977
8.067781947	7.85E-22	macrophage expressed 1, tandem duplicate 1	mpeg1.1	ZDB-GENE-030131-7347	335407
4.183893764	9.14E-22	CCAAT/enhancer binding protein (C/EBP), beta	cebpb	ZDB-GENE-020111-3	140814
9.25435495	6.52E-21	si:ch211-102c2.4	si:ch211-102c2.4	ZDB-GENE-030131-8862	568178
4.122049372	8.44E-21	fatty acid binding protein 11a	fabp11a	ZDB-GENE-040912-132	447944
4.958997926	1.18E-20	coronin, actin binding protein, 1 A	coro1a	ZDB-GENE-030131-9512	100002113
5.179139762	2.01E-20	Fc receptor, IgE, high affinity I, gamma polypeptide like	fcer1gl	ZDB-GENE-070502-4	100101653
7.846346992	3.41E-20	connexin 32.2	cx32.2	ZDB-GENE-050303-1	566647
4.234645883	4.88E-20	cathepsin C	ctsc	ZDB-GENE-030619-9	368704
4.507055275	5.17E-20	legumain	lgmn	ZDB-GENE-021030-1	406625
8.734468946	7.90E-20	GRB2-related adaptor protein a	grapa	ZDB-GENE-050522-347	553596
8.9405533	1.04E-19	interleukin-1 family member A	il1fma	ZDB-GENE-140106-231	102997062
6.437918568	1.35E-19	lectin, galactoside-binding, soluble, 3 binding protein b	lgals3bpb	ZDB-GENE-040426-2262	405809
8.410056881	1.51E-19	neutrophil cytosolic factor 1	ncf1	ZDB-GENE-031006-6	378966
7.080422693	2.03E-19	apoptosis facilitator Bcl-2-like protein 14	LOC101885512	NA	101885512
6.427189127	3.22E-19	chemokine (C-X-C motif) ligand 19	cxcl19	ZDB-GENE-140708-2	100003911
6.677182232	4.15E-19	integrin, beta 2	itgb2	ZDB-GENE-110411-4	557797
8.305047042	5.60E-19	si:dkey-88j15.3	si:dkey-88j15.3	ZDB-GENE-100922-28	560795
4.407928906	7.81E-19	GM2 ganglioside activator	gm2a	ZDB-GENE-050417-373	550529
4.341624501	1.03E-18	Rho GDP dissociation inhibitor (GDI) gamma	arhgdig	ZDB-GENE-040426-1493	394132
7.971312316	1.07E-18	si:cabz01074946.1	si:cabz01074946.1	ZDB-GENE-160113-134	100331505
7.338888853	1.15E-18	lysosomal-associated protein transmembrane 5	LOC100151049	NA	100151049
7.269771345	1.15E-18	protein tyrosine phosphatase, non-receptor type 6	ptpn6	ZDB-GENE-030131-7513	335573
9.665266832	2.03E-18	cytotoxic and regulatory T-cell molecule	crtam	NA	101884219
6.67300911	2.46E-18	tumor necrosis factor b (TNF superfamily, member 2)	tnfb	ZDB-GENE-050601-2	554167
5.681315201	1.12E-17	glutathione S-transferase omega 2	gsto2	ZDB-GENE-041114-67	492500
4.081012634	1.44E-17	sequestosome 1	sqstm1	ZDB-GENE-040426-2204	406452
6.184453342	1.62E-17	IL-6 subfamily cytokine M17	m17	ZDB-GENE-060526-368	555717

Table 1. Top 50 transcripts enriched in *mpeg1*:GFP+ cells compared to GFP− retinal cells at 7 days post ouabain lesion, sorted by FDR.

and digestion of engulfed material (for example, lysosome, phagosome, endocytosis), several innate immune receptors (for example, NOD-like receptor signaling pathway, Toll-like receptor signaling pathway, RIG-I-like receptor signaling pathway), and cytokine signaling (Cytokine-cytokine receptor interaction). In addition, Kegg analysis reveals enrichment in MAPK signaling pathway and Metabolic pathways.

Identification of candidate regeneration-associated transcripts in *mpeg1*:GFP+ cells.   One goal of our transcriptome analysis was to reveal transcriptional programs in microglia/macrophages that may be key to successful retinal regeneration. Since we were unable to sort GFP+ cells from undamaged (including saline injected) retinas due to the inability to collect sufficient numbers of GFP+ cells from the cell sorter[38], we qualitatively compared our list of transcripts enriched in GFP+ retinal cells (by at least log2FC > 2) during regeneration to transcripts identified by Oosterhof *et al.* to be enriched in steady-state zebrafish brain microglia (also by at least log2FC > 2) using the same *mpeg1*:GFP transgenic zebrafish and GFP−based sorting strategy[12]. This comparison was used to generate a collection of candidate genes with putatively enriched expression by microglia/macrophages in a regenerative environment. We used Ensembl IDs as a proxy to determine GFP+ enriched transcripts (with log2FC > 2) in both this study and that reported by Oosterhof *et al.*, only found to be enriched in *mpeg1*:GFP+ cells obtained from undamaged brains ("steady-state brain microglia"[12]), or only found to be enriched in *mpeg1*:GFP+ obtained from regenerating retinas (this study).

We found that 562 of our identified transcripts meeting this cut-off criteria were shared with steady-state brain microglia (Fig. 5A and Supplementary File S4), and Gene Ontology analysis placed the majority of these shared transcripts into categories representing known immune cell functions in pathogen response and phagocytic machinery (not shown) representative of core, signature genes associated with microglia and macrophages. These shared transcripts include several genes previously described in microglia (e.g. *slc7a7*, *p2ry12*, *irf8*[62,63,78]), as well as classes of genes such as granulins (e.g. *grna*, *grn1*), complement components (e.g. *c1qa*, *c1qb*, *c1qc*), cytokines (e.g. *il1b*, *tnfb*), and members of the TNF superfamily (e.g. *tnfsf12*, *tnfaip8l2b*, *tradd*). In addition, several novel transcripts identified by Oosterhof *et al.* in zebrafish brain microglia[12] were also common with our list of transcripts enriched in microglia/macrophages during retinal regeneration (e.g. *tmem104*, *rgs18*, *slc43a3b*, *plaua*).

In terms of transcripts found to be enriched with (cut-off of log2FC > 2) in microglia/macrophages in steady state[12] versus those found to be enriched in regenerative contexts (this study), our comparison revealed 1851 transcripts unique to *mpeg1*:GFP+ cells in the resting brain and 409 transcripts unique to *mpeg1*:GFP+ cells in regenerating retinas (Fig. 1A and Supplementary File S4, the latter now referred to as "regeneration-associated" transcripts), consistent with a significant shift in the transcriptional program of *mpeg1* expressing cells in the context of active neuronal regeneration. The reduced number of "regeneration-associated" transcripts compared to those from steady state brain could indicate a transcriptional program that is dedicated, at least transiently, to specialized functions in this unique biological context. In support of this idea, transcripts corresponding to toll-like receptor (*tlr*) genes, which comprise a core set of genes involved in detection and initiation of immune response to microbes[79], showed differential presence in steady-state *mpeg1*-expressing cells (17 *tlr* transcripts) compared to regeneration-associated transcripts (no *tlr* transcripts), with only one *tlr* transcript common between the two states (*tlr1*, Supplementary File S4). This could indicate a shift in dedication of microglia/macrophage function away from immune surveillance and towards other function(s) more appropriate for and dedicated to retinal regeneration at this timepoint. Interestingly, in contrast, upregulation of *tlr* gene expression is characteristic of microglia (and other glia) in several human neurodegenerative diseases[9].

To suggest alternative functions of microglia/macrophages during retinal regeneration compared to those in "steady-state" tissue, we performed GO analysis on the list of "regeneration-associated" transcripts, which revealed overrepresentation of categories including ATP hydrolysis coupled transport and protein transport (Biological Process, Molecular Funciton), categories related to GTPase activity and reglation (Molecular Function) and vacuolar V-type ATPase complex and endosome (Cellular Component) (Fig. 5B and Supplementary File S5). Together, these categories indicate that microglia/macrophages may be engaged in functions dedicated to active intracellular vesicle transport/fusion (perhaps both endocytic and exocytic) and vacuolar acidification of membrane bound compartments within the cell during retinal regeneration. Collectively, this suggests a phagocytic and/or exocytic function of microglia/macrophages during retinal regeneration. It is possible that neuronal debris from the initial insult remain at this timepoint; however, the 7dpi sampling time is several days later than the peak of neuronal cell death seen at ~1 dpi[18,31], and axon outgrowth from regenerating ganglion cells is detectable by 7 dpi[18]. Therefore, such a function may instead be involved with maintaining proper tissue conditions and integrity, and/or possibly release of secreted factors, although putative targets of phagocytosis and identity of such secreted factors remains an open-ended question.

Further comparisons of our list of GFP+ enriched transcripts during retinal regeneration to transcripts found by Oosterhof *et al.* to be upregulated, or downregulated, in *mpeg1*:GFP+ cells upon acute brain damage (again with log2FC > 2) revealed only 10, or 2, shared transcripts, respectively (Fig. 5C,D and Supplementary File S6). This suggests that *mpeg1* expressing cells present during active retinal regeneration possess a transcriptome that is substantially different than that of *mpeg1*+ cells responding to acute neuronal damage. This also further supports that the list of candidate "regeneration-associated" transcripts identified from the comparison to steady-state brain *mpeg1*:GFP+ cells (discussed above) represents a transcriptional program expressed by microglia/macrophages in a regenerative tissue state.

Discussion

Our analysis of regenerating retinal tissue following a tissue disrupting ouabain induced lesion (sparing photoreceptors) reveals that the inner nuclear layer of regenerating retinas contains *mpeg1*-expressing GFP+ immune cells, indicating that these cells identify as microglia/macrophages. These *mpeg1*+ cells appear ameboid in morphologies that often conform to the network of reactive Müller glia. Rather than showing regular distribution throughout retinal tissue, *mpeg1*+ cells are irregularly dispersed and mainly localize to basal regions of regenerating retinal tissues, possibly excluded from regions of MG-derived neuronal progenitor proliferation that occurs when MG-derived progenitors migrate apically towards the outer nuclear layer[19,52,80]. This distribution indicates that localization of *mpeg1*+ cells within regenerating retinal tissue could be spatially regulated. From our analysis

moderated log2FC	FDR	GENE NAME	SYMBOL	ZFIN	ENTREZID
−9.902497402	4.52E-39	prostaglandin D2 synthase b, tandem duplicate 2	ptgdsb.2	ZDB-GENE-030911-3	751701
−5.354755121	1.18E-29	arrestin 3a, retinal (X-arrestin)	arr3a	ZDB-GENE-040718-102	436678
−8.788432384	4.96E-27	biglycan b	bgnb	ZDB-GENE-040426-21	792197
−5.457182226	3.46E-24	phosphodiesterase 6 H, cGMP-specific, cone, gamma, paralog a	pde6ha	ZDB-GENE-040426-1754	393758
−5.100382872	1.57E-23	guanine nucleotide binding protein (G protein), beta polypeptide 3b	gnb3b	ZDB-GENE-040426-2280	406483
−9.975719622	1.35E-22	ba1 globin	ba1	ZDB-GENE-990415-18	30216
−5.337784049	1.35E-22	recoverin 2	rcvrn2	ZDB-GENE-030131-7590	335650
−6.435756586	1.46E-22	guanine nucleotide binding protein (G protein), gamma transducing activity polypeptide 2b	gngt2b	ZDB-GENE-091020-4	797361
−6.397569387	8.07E-22	opsin 1 (cone pigments), short-wave-sensitive 1	opn1sw1	ZDB-GENE-991109-25	30582
−6.09923235	8.44E-21	phosphodiesterase 6 C, cGMP-specific, cone, alpha prime	pde6c	ZDB-GENE-040426-1664	393845
−8.761307281	1.03E-19	ral guanine nucleotide dissociation stimulator-like 3a	rgl3a	ZDB-GENE-101130-1	100149956
−7.8244016	1.77E-19	MYCN proto-oncogene, bHLH transcription factor	mycn	ZDB-GENE-020711-1	252851
−6.044518098	2.44E-19	insulin-like growth factor binding protein 5b	igfbp5b	ZDB-GENE-040319-2	403039
−8.029031786	3.45E-19	solute carrier family 38, member 4	slc38a4	ZDB-GENE-041010-14	449771
−5.288624547	3.45E-19	aquaporin 1a (Colton blood group), tandem duplicate 1	aqp1a.1	ZDB-GENE-030131-7764	335821
−5.836694213	6.71E-19	guanine nucleotide binding protein (G protein), gamma transducing activity polypeptide 2a	gngt2a	ZDB-GENE-030131-7595	335655
−7.439163089	1.13E-18	NA	NA	NA	NA
−4.079039413	1.45E-18	fatty acid binding protein 7, brain, a	fabp7a	ZDB-GENE-000627-1	58128
−6.971250125	3.09E-18	solute carrier family 24 (sodium/potassium/calcium exchanger), member 2	slc24a2	ZDB-GENE-060825-277	751686
−8.382635563	6.75E-18	unc-119 homolog b (C. elegans)	unc119b	ZDB-GENE-050201-2	678653
−8.363908429	1.26E-17	follistatin b	fstb	ZDB-GENE-031118-139	566538
−8.099791471	1.44E-17	espin	espn	ZDB-GENE-081105-173	567061
−7.466759677	4.39E-17	fatty acid desaturase 2	fads2	ZDB-GENE-011212-1	140615
−4.673096962	6.59E-17	retinol binding protein 4, like	rbp4l	ZDB-GENE-030131-7591	335651
−6.617741567	1.62E-16	synaptotagmin Va	syt5a	ZDB-GENE-040718-110	436686
−6.853925862	1.83E-16	peripherin 2a (retinal degeneration, slow)	prph2a	ZDB-GENE-000616-8	58085
−4.326891	3.67E-16	midkine a	mdka	ZDB-GENE-990621-1	30277
−10.78175227	4.55E-16	T-box 2b	tbx2b	ZDB-GENE-990726-27	30253
−10.29982042	5.43E-16	si:ch211-183d21.1	si:ch211-183d21.1	ZDB-GENE-030131-8516	571430
−7.361502097	5.82E-16	doublecortin-like kinase 2a	dclk2a	ZDB-GENE-050420-170	572548
−10.57382742	6.16E-16	protein kinase C and casein kinase substrate in neurons 1a	pacsin1a	ZDB-GENE-050522-155	553559
−6.109615504	6.38E-16	zgc:195173	zgc:195173	ZDB-GENE-081022-190	792613
−10.29473981	7.27E-16	transmembrane protein 108	tmem108	ZDB-GENE-091204-397	563089
−5.473704873	1.73E-15	opsin 1 (cone pigments), long-wave-sensitive, 2	opn1lw2	ZDB-GENE-040718-141	436716
−7.717505976	2.51E-15	tight junction protein 2b (zona occludens 2)	tjp2b	ZDB-GENE-040718-58	436639
−8.088389566	5.77E-15	retinol binding protein 3	rbp3	ZDB-GENE-990415-132	30735
−8.358797824	6.92E-15	storkhead box 2a	stox2a	ZDB-GENE-090313-101	571741
−5.691417183	1.38E-14	ATPase, Na+/K+ transporting, alpha 1b polypeptide	atp1a1b	ZDB-GENE-001212-5	64616
−6.468437477	1.87E-14	collagen type XVIII alpha 1 chain a	col18a1a	ZDB-GENE-030516-3	564123
−5.409702873	2.17E-14	solute carrier family 1 (glial high affinity glutamate transporter), member 2b	slc1a2b	ZDB-GENE-030131-7779	335836
−8.857169039	2.50E-14	erythrocyte membrane protein band 4.1 like 5	epb41l5	ZDB-GENE-030616-450	368449
−7.392218598	3.00E-14	si:ch211-81a5.8	si:ch211-81a5.8	ZDB-GENE-060503-138	560648
−9.889739986	4.98E-14	BOC cell adhesion associated, oncogene regulated	boc	ZDB-GENE-030131-6560	334628
−9.997009725	5.09E-14	hairy-related 2	her2	ZDB-GENE-980526-274	30300
−7.35634514	5.33E-14	si:dkey-126g1.9	si:dkey-126g1.9	ZDB-GENE-030131-9862	792999
−10.86276442	9.44E-14	collagen, type V, alpha 2a	col5a2a	ZDB-GENE-030616-13	564821
−8.375593909	9.47E-14	shroom family member 2a	shroom2a	ZDB-GENE-050208-128	386817
−7.42402034	1.04E-13	NA	NA	NA	NA
−4.477364135	1.08E-13	ATPase, H+ transporting, lysosomal, V0 subunit cb	atp6v0cb	ZDB-GENE-030131-4127	325402
−10.42654367	1.69E-13	si:ch211-285j22.3	si:ch211-285j22.3	ZDB-GENE-141216-187	336034

Table 2. Top 50 transcripts depleted in *mpeg1*:GFP+cells compared to GFP− retinal cells at 7 days post ouabain lesion, sorted by FDR.

of cells expressing PCNA in regenerating retinal tissue at 7 dpi ouabain lesion, most of the PCNA signal can be attributed to reactive MG and MG-derived progenitors, indicating that most cell proliferation at this timepoint is to ultimately regenerate retinal neurons that were destroyed by the lesion. Based on PCNA staining alone, we

	qPCR transcript detection, Ct values		
Transcript	DE, RNA-seq	*mpeg1*:GFP+	GFP−	Fold expression, qPCR
lcp1	+6.18	29.36	unreliable§	N/A
mpeg1.1	+8.07	29.90	unreliable	N/A
p2ry12	+8.69	27.17	30.61	67.87
itgb2	+6.68	29.60	33.10	45.08
apoc1	+6.95	23.99	25.80	30.29
c1qa	+5.84	28.40	31.50	35.01
c1qb	+5.62	32.40	unreliable	N/A
cfp	+4.03	30.06	unreliable	N/A
il1b	+5.53	31.20	unreliable	N/A
lgals3bpb	+6.45	22.73	27.39	102.98
18 s		26.83	24.86	

Table 3. qPCR validation of selected transcripts found to be enriched in GFP+ compared to GFP− populations. §Unreliable: Average Ct value ≥ 34 (indicating single copy levels) and/or Ct value reported as "undetermined" by the instrument for at least 2 of 3 samples. N/A: Not applicable.

	qPCR transcript detection, Ct values		Fold expression, qPCR
Transcript	DE, RNA-seq	*mpeg1*:GFP+	GFP−	
crx	−3.82	31.10	27.19	0.30
opn1lw2	−5.47	not detected‡	22.24	N/A
gfap	−4.70	unreliable§	31.60	N/A
pax6a	−4.24	unreliable	30.33	N/A
ascl1a	−4.59	not detected	32.12	N/A
mef2ca	−3.80	not detected	30.76	N/A
ncam1b	−2.82	30.58	26.82	0.60
sept8b	−8.97	33.30	28.81	0.19
pdca	−6.92	not detected	26.70	N/A
prom1b	−7.25	not detected	29.41	N/A
18 s		26.83	24.86	

Table 4. qPCR validation of selected transcripts found to be depleted in GFP+ compared to GFP− populations. ‡Not detected: Ct value reported as "undetermined" by the instrument for all samples. §Unreliable: Average Ct value ≥ 34 (indicating single copy levels) and/or Ct value reported as "undetermined" by the instrument for at least 2 of 3 samples. N/A: Not applicable.

cannot exclude that at least some *mpeg1+* cells are also proliferative, since PCNA signal was occasionally associated with both L-plastin and GS. Differentially expressed genes (based on our cut-off criteria) did not show enrichment in GO categories associated with cell division for *mpeg1+* cells; however, the GFP− population contains proliferative MG and progenitors, therefore differential gene expression analysis would not reveal such transcripts.

In regenerating retinas, the density of immune cells is reduced with distance from the optic nerve head. The reason for this spatial distribution remains unknown. Interestingly, a recent report documented repopulation of homeostatic microglia in a mouse model system revealing a pattern of microglial repopulation that started in central retina and then spread peripherally[81]. However, any repopulation of zebrafish microglia has yet to be demonstrated. In addition, several genes found to be enriched in our study, but not in steady-state microglia[12] (Fig. 5), may represent orthologues to mammalian genes that may be involved in monocyte to macrophage differentiation (*mafbb*[82,83], *runx3*[84–86], *bhlhe40*[87], *bhlhe41*[87,88]) or macrophage chemoattraction (*cd4-1*, *il16*[89–91]), suggesting that retinas collected at the timepoint in this study may contain other macrophage populations. We are unable to distinguish between CNS microglia and other macrophages based on current markers in zebrafish, so other experimental approaches will need to be employed to determine if either of these are the case.

In addition, the dense network of immune cells at the optic nerve head could represent locations of microglia/macrophage function, such as phagocytosis of debris. Although markers of cell death are only minimally detected at 7 dpi following inner retinal ouabain-induced lesion[18], cellular and/or tissue debris may remain. By 7 dpi, ganglion cell-associated gene expression has mostly recovered[21] and ganglion cell markers indicate axon outgrowth occurs by this timepoint[18]. Microglia/macrophages could be involved in functions related to ganglion cell axon regeneration and re-connection to the onh, which are likely required to restore functional vision. However, the time at which axons reach the optic nerve head has not been determined and has been documented only at 21 dpi[21]. Further, microglia have been shown to prune ganglion cell axons during development in mice[2], and microglia/macrophages are activated within the vicinity of damage following injury to ganglion cell axons in

Gene	Sense (forward) 5′→3′	Anti-sense (reverse) 5′→3′
lcp1	GCAGTGGGTGAACGAAACAC	TCGAGATCGCATACTTGGCG
mpeg1.1	CATGTCGTGGCTGGAACAGA	ATGGTTACGGACTTGAACCCG
p2ry12	AGCGTCTCCAACAGTTCATCC	GCCAGAGCGTTCAGGGATAATC
itgb2	TGCTGGTAAAGACCCAGTGC	TTTGGGGCATCCCTGGTCTA
c1qa	TGACAGCGAGACACTGATGTT	GCGCCATTTCTTCCATGCTT
c1qb	GATCCAGGTGAGAATGCAGTG	TCCCTCTGGTCCCTTCACAC
apoc1	AAGACCAAAACCGCCTTCCA	GGGGGTGTAAGGTAAATGGGG
il1b	TTCCCCAAGTGCTGCTTATT	AAGTTAAAACCGCTGTGGTCA
cfp	TCCTCAGCCTGCTCTGTGACTTGTG	TTCGGGTTCCCTCCCTGGTTCT
lgals3bpb	GGTGGACATCAGCCAGACTT	CCAGCTGATGGAGACACTGA
crx	CATAACTGGAGGGGAATCTG	AAAGCACGACACAAGAACTC
pax6a	CACATACACACCCCCGCAC	CCGAGGCGGCCATTG
ascl1a	GCCAGACGGAACGAGAGAGA	AGGGTTGCAAAGCCGTTG
gfap	CTAAGCCAGACTTGACCGCT	TTACGATTGGCTGCATCCGT
opn1lw2	AGAGGGAAGAACTGGACTTTCAGA	TTCAGAGGAGTTTTGCCTACATATGT
mef2ca	TGTAATCATTCAGCGTAGTG	TCTAAGGTGTGCCGTTAT
ncam1b	AGTTTGATAAAGATGTTCGTTTC	TTAATGCTGCGGAAGTCA
sept8b	CTATCGTGGACTACATTGA	ATGAAGTACAGGCAGATG
pdca	TGCCGATGTGGAATAATCAGA	ACAGCGTCATTACTCATTCTATCT
prom1b	CAGTTGGAGTGACAGTTG	TCAGGTCTCTTATGTTGGT
18 s	GAACGCCACTTGTCCCTCTA	GTTGGTGGAGCGATTTGTCT

Table 5. Primer sequences used for qPCR.

other systems[92–94], although their functions in this context remain unclear[95]. Further work towards understanding microglial function during regeneration will in turn accelerate progress toward applying regenerative strategies to repair damaged or diseased human retina, including reestablishment of ganglion cell axons[96–98].

To our knowledge, this is the first work to use RNA sequencing to probe the transcriptome of microglia/macrophages isolated from CNS tissue engaged in a regenerative state. We provide here a list of hundreds of genes enriched in *mpeg1*-expressing cells obtained from highly pure cell populations at a key timepoint during active retinal regeneration in zebrafish. We provide strong evidence that this list of transcripts indeed represents the indicated populations in the desired context, although the *mpeg1+* may be composed of heterogeneous macrophage cell types (e.g. microglia along with macrophages originating from other sources and/or in distinct phenotypic states). Overall, this dataset provides a novel and exciting resource to the scientific community that will facilitate discovery of microglia/macrophage-specific factors that are crucial to the identity and specification of these immune cell populations (thus potentially leading to identification of better microglia and/or macrophage specific markers) and importantly, identification of factors that function during retinal (and possibly more globally, CNS) regeneration. This dataset will also help to advance our understanding of microglia and macrophage populations in a variety of model organisms.

Our dataset of *mpeg1*:GFP+ enriched transcripts likely represents genes that specify/identify microglia/macrophage cell lineage and may also include genes that have functional roles during regeneration. Therefore, it is important to identify which of these transcripts are specific to the context of retinal regeneration. Due to the inability to sort sufficient numbers of GFP+ cells from control (undamaged or saline injected) retinas with the number of pooled retinas used in this study[38], we compared our dataset to Oosterhof *et al.* (brain microglia[12], discussed in Results above). Using this strategy, we identified several hundred genes that may be enriched in microglia/macrophages during active regeneration. It is also worth restating that this list was generated using a cut-off of log2FC > 2, therefore the list of candidate "regeneration associated" transcripts likely includes transcripts that are not expressed in microglia in steady-state as well as those that are putatively upregulated in microglia/macrophages in a regenerative context. Although differences in sequencing methods, the identity of the GFP− population, and analysis methods are a caveat of such a comparison across studies, the high number of genes found to be unique to our study, and changes in categories of genes such as those coding for toll-like receptors and v-ATPase subunits, indicates that the transcriptome of *mpeg1+* cells in a regenerative tissue environment is significantly different than that of steady-state microglia, and of microglia/macrophages responding to acute neuronal damage. Therefore, this set of "regeneration-associated" transcripts is likely to yield a wealth of opportunity for probing individual candidate genes, and/or cellular pathways, for microglia and/or macrophage-specific functions during retinal (and CNS) regeneration.

Indeed, GO analysis suggests that *mpeg1* expressing cells in contexts of active retinal regeneration have specific functions that may involve vacuolar ATPase-coupled transport related to phagocytosis of extracellular substrates. In support of this, live imaging of microglial phagocytosis during zebrafish brain development indicates that v-type ATPases are involved with intracellular vesicle fusion after engulfment of apoptotic neurons[11] and a recent report indicates that microglia sense and ingest stressed neurons[99]. Although it remains to be determined, this dedicated function could be required to clean up cellular corpses and/or debris that arise during Müller
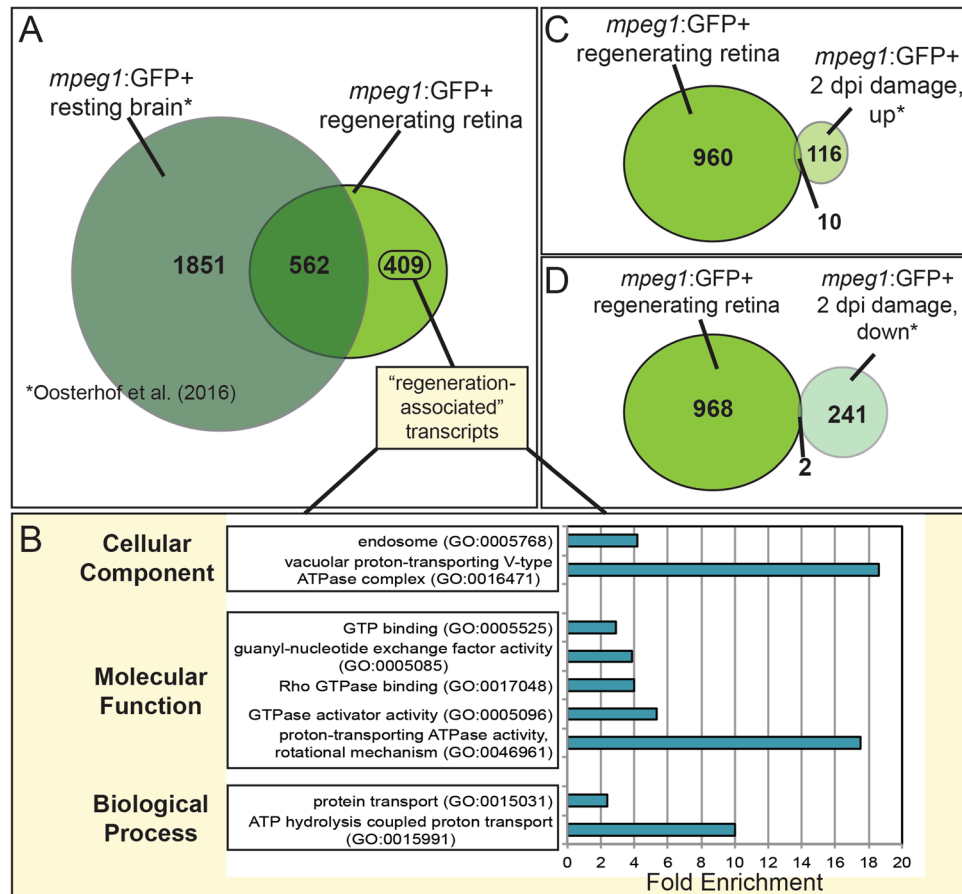
Figure 5. Identification of unique transcripts expressed by *mpeg1*:GFP+ cells during retinal regeneration. (**A**) The list of transcripts found to be enriched in *mpeg1*:GFP+ cells (log2FC > 2) during retinal regeneration (*mpeg1*:GFP+ regenerating retina, this study) was compared to that published to be enriched in *mpeg1*:GFP+ cells (log2FC > 2) obtained from steady-state (*mpeg1*:GFP+ resting brain, Oosterhof *et al.*[12]). "Regeneration-associated" transcripts (409 transcripts) are those found to be enriched in this study (with log2FC > 2), but not in *mpeg1*:GFP+ cells in steady-state brain (with log2FC > 2). (**B**) GO analysis of the 409 "regeneration-associated" transcripts shows enrichment of indicated categories in Cellular Component, Molecular Function, and Biological Process. P < 0.01 for all categories shown. (**C**) The list of transcripts found to be enriched in *mpeg1*:GFP+ cells in this study (again with log2FC > 2) was also compared to transcripts found to be upregulated or downregulated in *mpeg1*:GFP+ cells isolated from acutely damaged (with log2FC > 2, 2 dpi damage, up or down, (**C,D**) zebrafish brain (Oosterhof *et al.*[12]). Venn diagrams show the number of transcripts unique or shared between the two studies. Collectively, these comparisons indicate that microglia/macrophages adopt a unique transcriptional program in the context of retinal regeneration. dpi = days post injury.

glia-mediated neuronal regeneration, thus maintaining a tissue microenvironment that is supportive of regeneration. However, levels of cell death at 7 dpi are minimal compared to the initial lesion[18].

It is worth noting that the extent to which zebrafish brain and retinal microglia in any state are transcriptionally similar or different is not known. Therefore, some of these "regeneration-associated" genes could represent differences between these two types of CNS resident microglia (which would provide a starting point for such a comparison), in addition to regeneration-specific transcriptional programs. Thus, any "regeneration associated" candidate genes will need to be carefully analyzed in control conditions in any follow-up studies while also noting that the presence of transcript does not always equate protein expression. It is also worth noting that the nature of differential gene expression analysis may not reveal any transcripts that are equally or non-differentially expressed in both GFP+ and GFP− populations.

Our list of "regeneration-associated" transcripts may also provide a resource to probe similarities and differences between fish and mammalian microglia responding to neuronal degeneration or in contexts of gliosis. This could ultimately assist us in identifying key similarities and differences in immune cell-mediated factors that may impact the outcome of CNS/retinal regeneration. Such analysis will require careful interpretation of orthology between species as such comparisons may indicate orthologous genes based on protein family similarities that may or may not represent precisely shared functions, and the naming/numbering system in fish does not align with that used in mammals. For example, several chemokines and chemokine receptors were enriched in

zebrafish *mpeg1*:GFP+ cells in both the Oosterhof *et al.*[12] and our study. Chemokines and chemokine receptors are included in rapidly evolving gene clusters and have undergone additional diversification in zebrafish[100,101]. The use of tools to look for orthologues of these chemokine genes in mammals may not provide findings that are simple to interpret, since these chemokines/chemokine receptors may or may not represent well-characterized, and similarly numbered, chemokine genes in mouse or human.

This work has increased our knowledge of the gene expression profile of zebrafish *mpeg1*+ retinal cells isolated from tissue engaged in regeneration. Since Müller glia, Müller glia-derived progenitors and neurons, and microglia/macrophages appear to be the major, and possibly only, cell types present in tissue regions undergoing regeneration following retinal damage, it is essential to understand the contributions of microglia and macrophages to this process. The associated microglia/macrophage specific transcriptome presented here provides insight to a wealth of candidate genes and cellular pathways towards understanding such contributions and to allow comparative work in other model organisms. This foundational information will allow us to begin work to identify the function of microglia/macrophages during successful retinal/CNS regeneration.

Methods

Animals.
Procedures using zebrafish were performed in compliance with protocols approved by the University of Idaho Animal Care and Use Committee (IACUC). Zebrafish (*Danio rerio*) were maintained on a 14:10 light:dark cycle in 28.5 °C recirculating, monitored system water, housed and propagated according to[102]. The transgenic zebrafish line *mpeg1:GFP* (*gl22 Tg*, GFP expressed in microglia/macrophages[13,49]) used in these experiments was obtained from the Zebrafish International Resource Center (ZIRC). Fish used in these experiments were of both sexes, age 10–12 months.

Retinal Lesion.
Chemical lesioning of zebrafish retinas was performed by intravitreal injection of ouabain (estimated final concentration of 2 μM) in order to destroy inner retinal neurons and spare photoreceptors and Müller glia as reported in[18,21,31,48]. Briefly, a working stock of 40 μM ouabain (ouabain octahydrate, Sigma-Aldrich) was prepared in 0.65% sterile saline (NaCl) solution. Fish were anesthetized by immersion in tricaine solution and an incision was made across the cornea using a sapphire blade. A Hamilton syringe was inserted into the incision, guided behind the lens, and 0.4–0.6 μL of 40 μM ouabain solution was injected into the vitreal chamber. Volume injected was based on diameter of the eye (measured with calipers) and upon calculations based on geometry and volumes of the eye and lens, resulting in an estimated final intraocular concentration of 2 μM[18,103]. Lesions were unilateral; only the right eye was injected. During the procedure, fish were continuously flushed with tricaine solution. Immediately following the procedure, fish were returned to tanks with fresh system water. The right eyes of a separate group of fish were injected with 0.65% sterile saline (NaCl) solution, to serve as controls (same solution was used for saline injections and for preparation of ouabain solution for injection).

For the RNA sequencing experiment, 32 fish were injected in the right eye and upon tissue collection, eight retinas were pooled per sample to create four biological replicates for FACS sorting[38]. To obtain RNA for qRT-PCR confirmation of selected transcripts, 15 fish were injected in the right eye and upon tissue collection, five retinas were pooled/sample to create three biological replicates for FACS sorting. For collection of bulk RNA and tissue processing for retinal cryosections, five control (saline injected) and five ouabain injected fish were used for subsequent analyses.

Tissue Collection and Processing for Retinal Cryosections.
To prepare retinal cryosections, whole eyes were enucleated using fine forceps, transferred to PBS, and the lenses were removed. Eyes were then fixed in phosphate-buffered, 4% paraformaldehyde containing 5% sucrose for 1 hr at room temperature, washed in phosphate-buffered (pH = 7.4) 5% sucrose, and then washed in a graded series ending in 20% sucrose. The following day, tissues were embedded in blocks of a 1:2 solution of OCT embedding medium (Sakura Finetek) and phosphate-buffered, 20% sucrose, and frozen in isobutane, supercooled with liquid N_2. After freezing solid, tissues were sectioned at 5 micron thickness using a Leica CM3050 cryostat. After overnight desiccation, tissue sections on glass slides were stored at −20 °C until use.

Immunofluorescence.
To stain retinal cryosections, tissue sections (5 micron thickness) were blocked in 20% goat serum for 30 minutes at room temperature, incubated in primary antibody overnight, washed in PBST for at least 30 minutes, incubated in secondary antibody for 1 hour, and washed in PBST for at least 30 minutes. Slides were then mounted in Vectashield + DAPI (Vector Labs), covered with a coverslip, and sealed with clear nail polish. Primary antibodies and dilutions used: rabbit polyclonal anti-zebrafish L-plastin[50,51] (1:10,000, a kind gift of Dr. Michael Redd), rat anti-PCNA (16D10, 1:200, Chromotek), mouse anti-Glutamine Synthetase (1:1000, BD Transduction Laboratories). Secondary antibodies conjugated to Cy3 or Alexa-Fluor647 (Jackson ImmunoResearch) were used at 1:200 dilution.

Microscopy and Image Acquisition.
Imaging of fluorescently stained retinal sections was performed with a Nikon Andor spinning disk confocal microscope equipped with a Zyla sCMOS camera running Nikon Elements software. Imaging was performed using a 40X (oil immersion) objective. For stitched images of entire retinal cryosections, images were acquired at 40X magnification using the large stitched images feature in Nikon Elements software and stitched based on DAPI signal. Image processing and analysis was performed using FIJI (ImageJ). To quantify pixel intensity of L-plastin+ signal, a continuous line was drawn, with width covering retinal layers, originating at the optic nerve head (onh) and extending to the peripheral retinal tissue. The "plot profile" feature was used to create a plot of pixel intensity (corresponding to L-plastin+ signal) as a function of distance along the line, originating from the onh.

13

FACS Sorting of GFP+ and GFP− Populations From Regenerating Retinas. The protocol used for retinal tissue dissociation at 7 days-post ouabain injection (dpi) and subsequent FACS cell sorting was described in detail in Sun *et al.*[38]. Briefly, following dark adaption followed by retinal tissue dissociation, GFP+ and GFP− populations were isolated by FACS using a SONY Cell Sorter SH800 at Washington State University. The gating strategy for FACS was based on the GFP signal intensity of *mpeg1+* cells (GFP+ cells), as well as the scatter characteristics (forward scatter, FSC; and side scatter, SSC) of the target cells, and the same gating was used for all biological replicates. A 488 nm laser with 525/50 photomultiplier tube (PMT) was used by the cell sorter to illuminate GFP+ cells for GFP−based sorting.

RNA Isolation, 3′mRNA-seq Library Synthesis, and RNA Sequencing. RNA was extracted from sorted GFP+ and GFP− populations using NucleoSpin® RNA XS kit (Machery-Nagel) following the manufacturer's protocol. RNA samples were quantified and quality-checked on a Fragment Analyzer Automated CE System (Advanced Analytical) at the IBEST Genomics Resources Core, University of Idaho. RNA yields (~14 ng/sample for GFP+ and ~29 ng/sample for GFP− populations) and Fragment Analyzer results are reported in[38]. Libraries for sequencing were prepared using the Lexogen QuantSeq. 3′mRNA-Seq Library Prep Kit FWD using 16 cycles of PCR as per manufacturer instructions. The following steps were then performed prior to sequencing: (1) additional (non-method specified) bead cleanup (1:1 Magbio), (2) five additional cycles of PCR with KAPA library amplification kit (ABI), (3) additional (non-method specified) bead cleanup (1:1 Mabgio), (4) Fragment Analyzer QA, (5) pool equimolar amounts, (6) additional (non-method specified) bead cleanup (2 × 1:1 Mabgio), (7) Fragment Analzyer (QA), (8) five additional cycles PCR with KAPA library amplification kit (ABI). The QuantSeq. 3′-mRNA sequencing method is described in[104].

Reads were sequenced at the University of Oregon on a SE75 run using an Illumina HiSeq. 4000. Reads were demultiplexed by University of Oregon. Approximately 27–41 million reads were obtained per sample library, with the exception of one library, which nevertheless provides depth suitable for downstream analysis towards expression profiling[105,106], and therefore was included in the analysis to increase statistical power. Reads were quantified using Salmon v0.9.1 using the quasi-mapping-based mode, and using "–noLengthCorrection" setting[107] against the Ensembl release-90 *Danio rerio* transcriptome (GRCz10). Mapping rates were approximately 61–69% for all samples. Sample reads and mapping rate are summarized in Supplemental Table S1.

Differential Gene Expression Analysis. Analysis was carried out using methods derived from[108]. Briefly, data was imported into R (R Core Team (2017), https://www.R-project.org/) using tximport[108]. Differential expression analysis was then carried out using DESeq2[109], and moderated log2FC is reported to normalize for lowly expressed transcripts. Gene clustering ananlysis was performed using the WGCNA strategy and package[110], and the resulting analysis is summarized in Supplementary File S1.

Gene Ontology and KEGG Pathway Analysis. GO analysis was performed to identify over-represented GO terms for genes found to be enriched in GFP+ compared GFP− cells with criteria of log2FC > 0 and p < 0.1 using GOstats[111]. KEGG analysis was performed to identify over-represented KEGG pathways for genes found to be enriched in GFP+ versus GFP− cells using the kegga function within the Limma package[112]. Enriched categories shown are based on a cut off of p < 0.01. GO analysis of transcripts relevant to comparisons to Oosterhof *et al.*[12] was performed using the Gene Ontology Consortium GO Enrichment Analysis Tool (www.geneontology.org).

Quantitative PCR (qPCR). cDNA samples intended for quantitative PCR (qPCR) follow-up of RNA-seq hits, quality of purified RNA was analyzed using a Nanodrop spectrophotometer. cDNA was synthesized using Superscript® III First-Strand Synthesis kit (Invitrogen) using random hexamer primers. qPCR was performed using SYBR-Green PCR Master Mix with amplification run on a model 7900HT Fast Real-Time PCR System (Applied Biosystems, Inc.). Three technical replicates were performed for each biological replicate, and template cDNA was diluted 1:20 prior to addition to the qPCR reaction. Where appropriate, relative quantitation of gene expression between sorted *mpeg1*:GFP+ and GFP− samples was determined using the $2^{-\Delta\Delta Ct}$ method with *18 s* ribosomal gene as the endogenous reference gene. In cases where average Ct was found to be >34 for the samples analyzed, we consider this amplification to be unreliable because Cts in the range of 34–40 indicate transcript quantities that approach single copy level in the sample well, and the qPCR instrument manufacturer recommends against their use in analysis such as ΔΔCt. In several instances, Ct values were returned as "undetermined" by the qPCR instrument (indicating a Ct was not obtained from the sample well by cycle 40) for either the GFP+ or GFP− population. Primer sequences are shown in Table 5.

Data Availability
The RNAseq dataset generated and analyzed in the current study are available in the GEO repository (Accession GSE120467). The other datasets generated and analyzed during the current study are available from the corresponding author on reasonable request.

References
1. Wang, X. *et al.* Requirement for Microglia for the Maintenance of Synaptic Function and Integrity in the Mature Retina. *Journal of Neuroscience* **36**, 2827–2842 (2016).
2. Schafer, D. P. *et al.* Microglia Sculpt Postnatal Neural Circuits in an Activity and Complement-Dependent Manner. *Neuron* **74**, 691–705 (2012).
3. Paolicelli, R. C. *et al.* Synaptic Pruning by Microglia Is Necessary for Normal Brain Development. *Science* **333**, 1456–1458 (2011).
4. Stevens, B. *et al.* The classical complement cascade mediates CNS synapse elimination. *Cell* **131**, 1164–1178 (2007).
5. Parkhurst, C. N. *et al.* Microglia promote learning-dependent synapse formation through brain-derived neurotrophic factor. *Cell* **155**, 1596–1609 (2013).

6. Morsch, M. *et al*. *In vivo* characterization of microglial engulfment of dying neurons in the zebrafish spinal cord. *Front. Cell. Neurosci.* **9**, e90572–11 (2015).

7. Mazaheri, F. *et al*. Distinct roles for BAI1 and TIM-4 in the engulfment of dying neurons by microglia. *Nature. Communications* **5**, 1–11 (2014).

8. Nimmerjahn, A., Kirchhoff, F. & Helmchen, F. Resting microglial cells are highly dynamic surveillants of brain parenchyma *in vivo*. *Science* **308**, 1314–1318 (2005).

9. Amor, S. & Woodroofe, M. N. Innate and adaptive immune responses in neurodegeneration and repair. *Immunology* **141**, 287–291 (2014).

10. Amor, S., Puentes, F., Baker, D. & van der Valk, P. Inflammation in neurodegenerative diseases. *Immunology* **129**, 154–169 (2010).

11. Peri, F. & Nüsslein-Volhard, C. Live Imaging of Neuronal Degradation by Microglia Reveals a Role for v0-ATPase a1 in Phagosomal Fusion *In Vivo*. *Cell* **133**, 916–927 (2008).

12. Oosterhof, N. *et al*. Identification of a conserved and acute neurodegeneration-specific microglial transcriptome in the zebrafish. *Glia* **65**, 138–149 (2016).

13. Svahn, A. J. *et al*. Development of ramified microglia from early macrophages in the zebrafish optic tectum. *Devel Neurobio* **73**, 60–71 (2012).

14. Sieger, D. & Peri, F. Animal models for studying microglia: The first, the popular, and the new. *Glia* **61**, 3–9 (2012).

15. Ferrero, G. *et al*. Embryonic Microglia Derive from Primitive Macrophages and Are Replaced by cmyb-Dependent Definitive Microglia in. *Zebrafish. CellReports* **24**, 130–141 (2018).

16. Bernardos, R. L., Barthel, L. K., Meyers, J. R. & Raymond, P. A. Late-stage neuronal progenitors in the retina are radial Müller glia that function as retinal stem cells. *J. Neurosci.* **27**, 7028–7040 (2007).

17. Fausett, B. V. & Goldman, D. A role for alpha1 tubulin-expressing Müller glia in regeneration of the injured zebrafish retina. *J. Neurosci.* **26**, 6303–6313 (2006).

18. Fimbel, S. M., Montgomery, J. E., Burket, C. T. & Hyde, D. R. Regeneration of Inner Retinal Neurons after Intravitreal Injection of Ouabain in Zebrafish. *Journal of Neuroscience* **27**, 1712–1724 (2007).

19. Nagashima, M., Barthel, L. K. & Raymond, P. A. A self-renewing division of zebrafish Müller glial cells generates neuronal progenitors that require N-cadherin to regenerate retinal neurons. *Development* **140**, 4510–4521 (2013).

20. Thummel, R. *et al*. Characterization of Müller glia and neuronal progenitors during adult zebrafish retinal regeneration. *Experimental Eye Research* **87**, 433–444 (2008).

21. Sherpa, T. *et al*. Retinal regeneration is facilitated by the presence of surviving neurons. *Devel Neurobio* **74**, 851–876 (2014).

22. Cameron, D. A., Gentile, K. L., Middleton, F. A. & Yurco, P. Gene expression profiles of intact and regenerating zebrafish retina. *Mol. Vis.* **11**, 775–791 (2005).

23. McCurley, A. T. & Callard, G. V. Time Course Analysis of Gene Expression Patterns in Zebrafish Eye During Optic Nerve Regeneration. *J Exp Neurosci* **2010**, 17–33 (2010).

24. Eastlake, K. *et al*. Comparison of proteomic profiles in the zebrafish retina during experimental degeneration and regeneration. *Sci Rep* **7**, 44601 (2017).

25. Sifuentes, C. J., Kim, J.-W., Swaroop, A. & Raymond, P. A. Rapid, Dynamic Activation of Müller Glial Stem Cell Responses in Zebrafish. *Invest. Ophthalmol. Vis. Sci.* **57**, 5148–5160 (2016).

26. Qin, Z., Barthel, L. K. & Raymond, P. A. Genetic evidence for shared mechanisms of epimorphic regeneration in zebrafish. *Proc. Natl. Acad. Sci. USA* **106**, 9310–9315 (2009).

27. Bringmann, A. *et al*. Cellular signaling and factors involved in Müller cell gliosis: neuroprotective and detrimental effects. *Progress in Retinal and Eye Research* **28**, 423–451 (2009).

28. Bringmann, A. *et al*. Müller cells in the healthy and diseased retina. *Progress in Retinal and Eye Research* **25**, 397–424 (2006).

29. Gallina, D., Todd, L. & Fischer, A. J. A comparative analysis of MUller glia-mediated regeneration in the vertebrate retina. *Experimental Eye Research* **123**, 121–130 (2014).

30. Karlstetter, M. *et al*. Retinal microglia: just bystander or target for therapy? *Progress in Retinal and Eye Research* **45**, 30–57 (2015).

31. Mitchell, D. M., Lovel, A. G. & Stenkamp, D. L. Dynamic changes in microglial and macrophage characteristics during degeneration and regeneration of the zebrafish retina. *Journal of Neuroinflammation* **15**, 163 (2018).

32. Thomas, J. L., Ranski, A. H., Morgan, G. W. & Thummel, R. Reactive gliosis in the adult zebrafish retina. *Experimental Eye Research* **143**, 98–109 (2016).

33. Raymond, P. A., Barthel, L. K., Bernardos, R. L. & Perkowski, J. J. Molecular characterization of retinal stem cells and their niches in adult zebrafish. *BMC Developmental Biology* **6**, 36 (2006).

34. Wang, M., Ma, W., Zhao, L., Fariss, R. N. & Wong, W. T. Adaptive Müller cell responses to microglial activation mediate neuroprotection and coordinate inflammation in the retina. *Journal of Neuroinflammation* **8**, 173 (2011).

35. Fischer, A. J., Zelinka, C., Gallina, D., Scott, M. A. & Todd, L. Reactive microglia and macrophage facilitate the formation of Müller glia-derived retinal progenitors. *Glia* **62**, 1608–1628 (2014).

36. Wang, M. *et al*. Macroglia-microglia interactions via TSPO signaling regulates microglial activation in the mouse retina. *J. Neurosci.* **34**, 3793–3806 (2014).

37. White, D. T. *et al*. Immunomodulation-accelerated neuronal regeneration following selective rod photoreceptor cell ablation in the zebrafish retina. *Proc. Natl. Acad. Sci. USA* **114**, E3719–E3728 (2017).

38. Sun, C., Mitchell, D. M. & Stenkamp, D. L. Isolation of photoreceptors from mature, developing, and regenerated zebrafish retinas, and of microglia/macrophages from regenerating zebrafish retinas. *Experimental Eye Research* **177**, 130–144 (2018).

39. Mazzolini, J., Chia, K. & Sieger, D. Isolation and RNA Extraction of Neurons, Macrophages and Microglia from Larval Zebrafish Brains. *J Vis Exp* e57431, https://doi.org/10.3791/57431 (2018).

40. Oosterhof, N. *et al*. Colony-Stimulating Factor 1 Receptor (CSF1R) Regulates Microglia Density and Distribution, but Not Microglia Differentiation. *In Vivo. CellReports* **24**, 1203–1217.e6 (2018).

41. Bailey, T. J., Fossum, S. L., Fimbel, S. M., Montgomery, J. E. & Hyde, D. R. The inhibitor of phagocytosis, O-phospho-l-serine, suppresses MUller glia proliferation and cone cell regeneration in the light-damaged zebrafish retina. *Experimental Eye Research* **91**, 601–612 (2010).

42. Morris, A. C., Schroeter, E. H., Bilotta, J., Wong, R. O. L. & Fadool, J. M. Cone Survival Despite Rod Degeneration in XOPS-mCFP Transgenic Zebrafish. *Invest. Ophthalmol. Vis. Sci.* **46**, 4762–10 (2005).

43. Sherpa, T. *et al*. Ganglion cell regeneration following whole-retina destruction in zebrafish. *Devel Neurobio* **68**, 166–181 (2008).

44. Vihtelic, T. S. & Hyde, D. R. Light-induced rod and cone cell death and regeneration in the adult albino zebrafish (Danio rerio) retina. *J. Neurobiol.* **44**, 289–307 (2000).

45. Yurco, P. & Cameron, D. A. Responses of Müller glia to retinal injury in adult zebrafish. *Vision Research* **45**, 991–1002 (2005).

46. Ramachandran, R., Reifler, A., Parent, J. M. & Goldman, D. Conditional gene expression and lineage tracing of tuba1a expressing cells during zebrafish development and retina regeneration. *J. Comp. Neurol.* **518**, 4196–4212 (2010).

47. Powell, C., Cornblath, E., Elsaeidi, F., Wan, J. & Goldman, D. Zebrafish Müller glia-derived progenitors are multipotent, exhibit proliferative biases and regenerate excess neurons. *Nature Publishing Group* 1–10, https://doi.org/10.1038/srep24851 (2016).

48. McGinn, T. E. *et al*. Restoration of Dendritic Complexity, Functional Connectivity, and Diversity of Regenerated Retinal Bipolar Neurons in Adult Zebrafish. *J. Neurosci.* **38**, 120–136 (2018).

49. Ellett, F., Pase, L., Hayman, J. W., Andrianopoulos, A. & Lieschke, G. J. Mpeg1 promoter transgenes direct macrophage-lineage expression in zebrafish. *Blood* **117**, e49–e56 (2011).
50. Herbomel, P., Thisse, B. & Thisse, C. Ontogeny and behaviour of early macrophages in the zebrafish embryo. *Development* **126**, 3735–3745 (1999).
51. Le Guyader, D. *et al.* Origins and unconventional behavior of neutrophils in developing zebrafish. *Blood* **111**, 132–141 (2008).
52. Lahne, M., Li, J., Marton, R. M. & Hyde, D. R. Actin-Cytoskeleton- and Rock-Mediated INM Are Required for Photoreceptor Regeneration in the Adult Zebrafish Retina. *J. Neurosci.* **35**, 15612–15634 (2015).
53. Lieschke, G. J. *et al.* Zebrafish SPI-1 (PU.1) marks a site of myeloid development independent of primitive erythropoiesis: implications for axial patterning. *Developmental Biology* **246**, 274–295 (2002).
54. Liongue, C., Hall, C. J., O'Connell, B. A., Crosier, P. & Ward, A. C. Zebrafish granulocyte colony-stimulating factor receptor signaling promotes myelopoiesis and myeloid cell migration. *Blood* **113**, 2535–2546 (2009).
55. Su, F. *et al.* Differential regulation of primitive myelopoiesis in the zebrafish by Spi-1/Pu.1 and C/ebp1. *Zebrafish* **4**, 187–199 (2007).
56. Wittamer, V., Bertrand, J. Y., Gutschow, P. W. & Traver, D. Characterization of the mononuclear phagocyte system in zebrafish. *Blood* **117**, 7126–7135 (2011).
57. Zakrzewska, A. *et al.* Macrophage-specific gene functions in Spi1-directed innate immunity. *Blood* **116**, e1–e11 (2010).
58. Okunuki, Y. *et al.* Microglia inhibit photoreceptor cell death and regulate immune cell infiltration in response to retinal detachment. *Proc Natl Acad Sci USA* **115**, E6264–E6273 (2018).
59. Butovsky, O. *et al.* Identification of a unique TGF-β–dependent molecular and functional signature in microglia. *Nat Neurosci* **17**, 131–143 (2013).
60. Mass, E. *et al.* Specification of tissue-resident macrophages during organogenesis. *Science* **353**, aaf4238–aaf4238 (2016).
61. Gosselin, D. *et al.* Environment drives selection and function of enhancers controlling tissue-specific macrophage identities. *Cell* **159**, 1327–1340 (2014).
62. Sousa, C., Biber, K. & Michelucci, A. Cellular and Molecular Characterization of Microglia: A Unique Immune Cell Population. *Front Immunol* **8**, 198 (2017).
63. Rossi, F., Casano, A. M., Henke, K., Richter, K. & Peri, F. The SLC7A7 Transporter Identifies Microglial Precursors prior to Entry into the Brain. *Cell Reports* **11**, 1008–1017 (2015).
64. Chinen, A., Hamaoka, T., Yamada, Y. & Kawamura, S. Gene duplication and spectral diversification of cone visual pigments of zebrafish. *Genetics* **163**, 663–675 (2003).
65. Shen, Y.-C. & Raymond, P. A. Zebrafish cone-rod (crx) homeobox gene promotes retinogenesis. *Developmental Biology* **269**, 237–251 (2004).
66. Yokoyama, S. Molecular evolution of vertebrate visual pigments. *Progress in Retinal and Eye Research* **19**, 385–419 (2000).
67. Renninger, S. L., Gesemann, M. & Neuhauss, S. C. F. Cone arrestin confers cone vision of high temporal resolution in zebrafish larvae. *Eur J Neurosci* **33**, 658–667 (2011).
68. Zang, J., Keim, J., Kastenhuber, E., Gesemann, M. & Neuhauss, S. C. F. Recoverin depletion accelerates cone photoresponse recovery. *Open Biol* **5**, 150086 (2015).
69. Mulligan, T., Blaser, H., Raz, E. & Farber, S. A. Prenylation-deficient G protein gamma subunits disrupt GPCR signaling in the zebrafish. *Cell. Signal.* **22**, 221–233 (2010).
70. Bayés, À. *et al.* Evolution of complexity in the zebrafish synapse proteome. *Nature Communications* **8**, 14613 (2017).
71. Gramage, E., D'Cruz, T., Taylor, S., Thummel, R. & Hitchcock, P. F. Midkine-a protein localization in the developing and adult retina of the zebrafish and its function during photoreceptor regeneration. *PLoS ONE* **10**, e0121789 (2015).
72. Calinescu, A.-A., Vihtelic, T. S., Hyde, D. R. & Hitchcock, P. F. Cellular expression of midkine-a and midkine-b during retinal development and photoreceptor regeneration in zebrafish. *J. Comp. Neurol.* **514**, 1–10 (2009).
73. Ramachandran, R., Zhao, X.-F. & Goldman, D. Ascl1a/Dkk/beta-catenin signaling pathway is necessary and glycogen synthase kinase-3beta inhibition is sufficient for zebrafish retina regeneration. *Proc. Natl. Acad. Sci. USA* **108**, 15858–15863 (2011).
74. Ramachandran, R., Fausett, B. V. & Goldman, D. Ascl1a regulates Müller glia dedifferentiation and retinal regeneration through a Lin-28-dependent, let-7 microRNA signalling pathway. *Nat. Cell Biol.* **17**, 532–532 (2015).
75. Wan, J. & Goldman, D. Opposing Actions of Fgf8a on Notch Signaling Distinguish Two Muller Glial Cell Populations that Contribute to Retina Growth and Regeneration. *CellReports* **19**, 849–862 (2017).
76. Elsaeidi, F. *et al.* Notch Suppression Collaborates with Ascl1 and Lin28 to Unleash a Regenerative Response in Fish Retina, But Not in Mice. *J. Neurosci.* **38**, 2246–2261 (2018).
77. Conner, C., Ackerman, K. M., Lahne, M., Hobgood, J. S. & Hyde, D. R. Repressing Notch Signaling and Expressing TNF Are Sufficient to Mimic Retinal Regeneration by Inducing Muller Glial Proliferation to Generate Committed Progenitor Cells. *Journal of Neuroscience* **34**, 14403–14419 (2014).
78. Nayak, D., Roth, T. L. & McGavern, D. B. Microglia development and function. *Annu. Rev. Immunol.* **32**, 367–402 (2014).
79. Kawasaki, T. & Kawai, T. Toll-like receptor signaling pathways. *Front Immunol* **5**, 461 (2014).
80. Lahne, M. & Hyde, D. R. Interkinetic Nuclear Migration in the Regenerating Retina. *Adv. Exp. Med. Biol.* **854**, 587–593 (2016).
81. Zhang, Y. *et al.* Repopulating retinal microglia restore endogenous organization and function under CX3CL1-CX3CR1 regulation. *Sci Adv* **4**, eaap8492 (2018).
82. Bakri, Y. *et al.* Balance of MafB and PU.1 specifies alternative macrophage or dendritic cell fate. *Blood* **105**, 2707–2716 (2005).
83. Kelly, L. M., Englmeier, U., Lafon, I., Sieweke, M. H. & Graf, T. MafB is an inducer of monocytic differentiation. *EMBO J.* **19**, 1987–1997 (2000).
84. Sánchez-Martín, L. *et al.* The chemokine CXCL12 regulates monocyte-macrophage differentiation and RUNX3 expression. *Blood* **117**, 88–97 (2011).
85. Estecha, A., Aguilera-Montilla, N., Sánchez-Mateos, P. & Puig-Kröger, A. RUNX3 regulates intercellular adhesion molecule 3 (ICAM-3) expression during macrophage differentiation and monocyte extravasation. *PLoS ONE* **7**, e33313 (2012).
86. Dong, C. *et al.* RNA sequencing and transcriptomal analysis of human monocyte to macrophage differentiation. *Gene* **519**, 279–287 (2013).
87. Saeed, S. *et al.* Epigenetic programming of monocyte-to-macrophage differentiation and trained innate immunity. *Science* **345**, 1251086–1251086 (2014).
88. Tserel, L. *et al.* Genome-wide promoter analysis of histone modifications in human monocyte-derived antigen presenting cells. *BMC Genomics* **11**, 642 (2010).
89. Takizawa, F. *et al.* Novel Teleost CD4-Bearing Cell Populations Provide Insights into the Evolutionary Origins and Primordial Roles of CD4+ Lymphocytes and CD4+ Macrophages. *J. Immunol.* **196**, 4522–4535 (2016).
90. Cruikshank, W. W. *et al.* Molecular and functional analysis of a lymphocyte chemoattractant factor: association of biologic function with CD4 expression. *Proc Natl Acad Sci USA* **91**, 5109–5113 (1994).
91. Cruikshank, W. W., Berman, J. S., Theodore, A. C., Bernardo, J. & Center, D. M. Lymphokine activation of T4+ T lymphocytes and monocytes. *The Journal of Immunology* **138**, 3817–3823 (1987).
92. Yin, Y. *et al.* Macrophage-derived factors stimulate optic nerve regeneration. *J. Neurosci.* **23**, 2284–2293 (2003).
93. Wohl, S. G., Schmeer, C. W., Witte, O. W. & Isenmann, S. Proliferative response of microglia and macrophages in the adult mouse eye after optic nerve lesion. *Invest. Ophthalmol. Vis. Sci.* **51**, 2686–2696 (2010).

94. Davis, B. M., Salinas-Navarro, M., Cordeiro, M. F., Moons, L. & De Groef, L. Characterizing microglia activation: a spatial statistics approach to maximize information extraction. *Sci Rep* **7**, 1576 (2017).
95. Hilla, A. M., Diekmann, H. & Fischer, D. Microglia Are Irrelevant for Neuronal Degeneration and Axon Regeneration after Acute Injury. *J. Neurosci.* **37**, 6113–6124 (2017).
96. Burns, M. E. & Stevens, B. Report on the National Eye Institute's Audacious Goals Initiative: Creating a Cellular Environment for Neuroregeneration. *Eneuro* **5**, ENEURO.0035–18.2018 (2018).
97. Jorstad, N. L. *et al.* Stimulation of functional neuronal regeneration from Müller glia in adult mice. *Nature* **548**, 103–107 (2017).
98. Yao, J. *et al.* Inhibiting autophagy reduces retinal degeneration caused by protein misfolding. *Autophagy* **14**, 1226–1238 (2018).
99. Zhao, L. *et al.* Microglial phagocytosis of living photoreceptors contributes to inherited retinal degeneration. *EMBO Mol Med* **7**, 1179–1197 (2015).
100. DeVries, M. E. *et al.* Defining the origins and evolution of the chemokine/chemokine receptor system. *The Journal of Immunology* **176**, 401–415 (2006).
101. Nomiyama, H. *et al.* Extensive expansion and diversification of the chemokine gene family in zebrafish: Identification of a novel chemokine subfamily CX. *BMC Genomics* **9**, 222–19 (2008).
102. Westerfield, M. *The Zebrafish Book. A Guide for the Laboratory Use of Zebrafish (Danio rerio), 5th edition.* (2007).
103. Raymond, P. A., Reifler, M. J. & Rivlin, P. K. Regeneration of goldfish retina: rod precursors are a likely source of regenerated cells. *J. Neurobiol.* **19**, 431–463 (1988).
104. Moll, P., Ante, M., Seitz, A. & Reda, T. QuantSeq. 3′mRNA sequencing for RNA quantification. *Nat. Methods* **11**, i–iii (2014).
105. Lohman, B. K., Weber, J. N. & Bolnick, D. I. Evaluation of TagSeq, a reliable low-cost alternative for RNAseq. *Mol Ecol Resour* **16**, 1315–1321 (2016).
106. Conesa, A. *et al.* A survey of best practices for RNA-seq data analysis. *Genome Biol.* **17**, 13 (2016).
107. Patro, R., Duggal, G., Love, M. I., Irizarry, R. A. & Kingsford, C. Salmon provides fast and bias-aware quantification of transcript expression. *Nat. Methods* **14**, 417–419 (2017).
108. Soneson, C., Love, M. I. & Robinson, M. D. Differential analyses for RNA-seq: transcript-level estimates improve gene-level inferences. *F1000Res* **4**, 1521 (2015).
109. Love, M. I., Huber, W. & Anders, S. Moderated estimation of fold change and dispersion for RNA-seq data with DESeq2. *Genome Biol.* **15**, 550 (2014).
110. Langfelder, P. & Horvath, S., Fast R Functions for Robust Correlations and Hierarchical Clustering. *J Stat Softw* **46** (2012).
111. Falcon, S. & Gentleman, R. Using GOstats to test gene lists for GO term association. *Bioinformatics* **23**, 257–258 (2007).
112. Ritchie, M. E. *et al.* limma powers differential expression analyses for RNA-sequencing and microarray studies. *Nucleic Acids Res.* **43**, e47–e47 (2015).

Acknowledgements

Author Contributions

D.M.M. designed and performed experiments, analyzed data, prepared figures, and wrote the manuscript. C.S. designed and performed experiments. S.S.H. participated in experimental design and performed bioinformatics analysis. D.D.N. participated in experimental design and RNAseq library preparation. D.L.S. designed experiments, analyzed data, and wrote the manuscript. All authors reviewed the manuscript.

Additional Information

Supplementary information accompanies this paper at https://doi.org/10.1038/s41598-019-41298-8.

Competing Interests: The authors declare no competing interests.

Publisher's note: Springer Nature remains neutral with regard to jurisdictional claims in published maps and institutional affiliations.